Phytopathology Research

RESEARCH Open Access

Identification of a novel C6 protein encoded by tomato leaf curl China virus

Zhiyuan Wang[1,2], Yaqin Wang[1], Rosa Lozano-Duran[3], Tao Hu[1*] and Xueping Zhou[1,2*]

Abstract

Begomoviruses cause significant losses to a wide range of crops worldwide, and a great progress has been made in characterizing some noncanonical proteins encoded by begomoviruses. In the present study, a novel viral protein, C6, was detected in *Nicotiana benthamiana* plants infected with tomato leaf curl China virus (ToLCCNV). Sequence analyses revealed that the C6 ORF is on the complementary strand of approximately 36% reported begomovirus sequences with conserved amino acid sequence. ToLCCNV C6 specifically localizes to mitochondria. Analysis of deletion mutants showed that C6 possesses an internal mitochondrial targeting signal. Overall, these data uncover a novel begomovirus-encoded protein targeting distinct plant cell organelles.

Keywords: Begomovirus, C6 protein, Mitochondrion targeting

Background

Members of the genus *Begomovirus* in the family *Geminiviridae* are plant-infecting DNA viruses that cause significant losses to a wide range of agronomic and horticultural crops worldwide (Hanley-Bowdoin et al. 2013). Begomoviruses are transmitted by the whitefly *Bemisia tabaci* (Hemiptera: Aleyrodidae), and over 400 species have been identified in the genus so far (Brown et al. 2015; Fiallo-Olivé et al. 2021). Based on geographic distribution and phylogenetic studies, begomoviruses can be broadly divided into the Old World (Eastern hemisphere) and the New World (Western hemisphere) groups (Rybicki 1994). According to genome organization and sequence similarity, begomoviruses can be further clustered into monopartite and bipartite (Zerbini et al. 2017). The genome of monopartite begomoviruses comprises a circular single-stranded DNA (ssDNA) molecule of approximately 2.6 kb, encoding a viral coat protein (CP), a V2 protein, a replication-associated protein (Rep/C1), a transcription activator protein (TrAP/C2), a replication enhancer protein (REn/C3), and a C4 protein (Sunter and Bisaro 1991, 1992; Laufs 1995; Pooma and Petty 1996; Rojas et al. 2001; Fondong 2013). The genome of bipartite begomoviruses contains two DNA components, each of approximately 2.6 kb, referred to as DNA-A and DNA-B. The DNA-A component is equivalent to the genome of monopartite begomoviruses, while the DNA-B component encodes a nuclear shuttle protein (NSP) and a cell-to-cell movement protein (MP) (Lazarowitz and Beachy 1999; Hanley-Bowdoin et al. 2000). In addition, begomoviruses are known to be frequently associated with different types of satellite ssDNA molecules that participate in virus infection and symptom development (Zhou 2013; Li et al. 2018; Yang et al. 2019).

In recent years, a series of studies have revealed that in addition to the well-documented proteins, begomoviruses encode some noncanonical small accessary proteins during the infection (Fontenelle et al. 2007; Hu et al. 2020; Li et al. 2021; Chiu et al. 2022). For example, mungbean yellow mosaic India virus (MYMIV) encodes an AC5 protein of 9.2 kDa to facilitate infection through suppressing host post-transcriptional gene silencing (PTGS) and transcriptional gene silencing (TGS) (Li et al. 2015). A cis-Golgi localized V3 protein of 9.3 kDa,

*Correspondence: taohu1989@zju.edu.cn; zzhou@zju.edu.cn

[1] State Key Laboratory of Rice Biology, Institute of Biotechnology, Zhejiang University, Hangzhou 310058, China
Full list of author information is available at the end of the article

encoded by tomato yellow leaf curl virus (TYLCV), is required for efficient virus cell-to-cell movement (Gong et al. 2021, 2022). These findings collectively provide insight into the infection details of geminiviruses, suggesting the involvement of more, yet-to-be characterized open reading frames (ORFs). To further investigate the molecular feature of begomovirus genomes, we focused on ORFs that have been neglected due to the small sizes using tomato leaf curl China virus (ToLCCNV) as a model. Here, an unexplored ORF in the complementary strand of the ToLCCNV genome, referred to as C6, was identified and characterized.

Results

Identification of a begomovirus-encoded C6 protein

From the total protein of *Nicotiana benthamiana* plants infected with ToLCCNV (GenBank: AJ558119) alongside with its betasatellite ToLCCNB (GenBank: AJ704612), we recovered unique peptides corresponding to a novel virus protein through mass spectrometry (MS) analysis (Fig. 1a, b). The identified ORF, designated as ToLCCNV C6, is in the complementary sense of the virus genome, partially overlaps with the CP and V2 ORFs, and encodes a polypeptide of 97 amino acids (Fig. 1c). To confirm that the C6 ORF was transcribed during the virus infection, the 556 bp ToLCCNV sequence upstream of the C6 translation initiation site was fused to the 5'-end of the green fluorescent protein (GFP) reporter gene. An *Agrobacterium tumefaciens* strain harboring the resulting construct (pC6 (556)-GFP) was infiltrated in *N. benthamiana* leaves with a promoter-less negative control (pCambia-GFP) and a cauliflower mosaic virus 35S promoter positive control (35S-GFP). Western blot analysis showed that the C6 upstream sequence could drive GFP expression (Fig. 1d). To better determine the promoter activity of C6 upstream sequence in the context of the virus infection, *N. benthamiana* leaves were infiltrated with *A. tumefaciens* harboring pC6 (556)-GFP together with ToLCCNV/ToLCCNB infectious clones or empty vector (pBinplus). Confocal microscopy showed enhanced GFP fluorescence in *N. benthamiana* leaves co-infiltrated with pC6 (556)-GFP and ToLCCNV/ToLCCNB (Fig. 1e). Consistent with this, Western blot analysis showed higher GFP protein accumulation in *N. benthamiana* leaves co-infiltrated with pC6 (556)-GFP and ToLCCNV/ToLCCNB compared with that in the control (co-infiltrated with pBinplus and pC6 (556)-GFP),

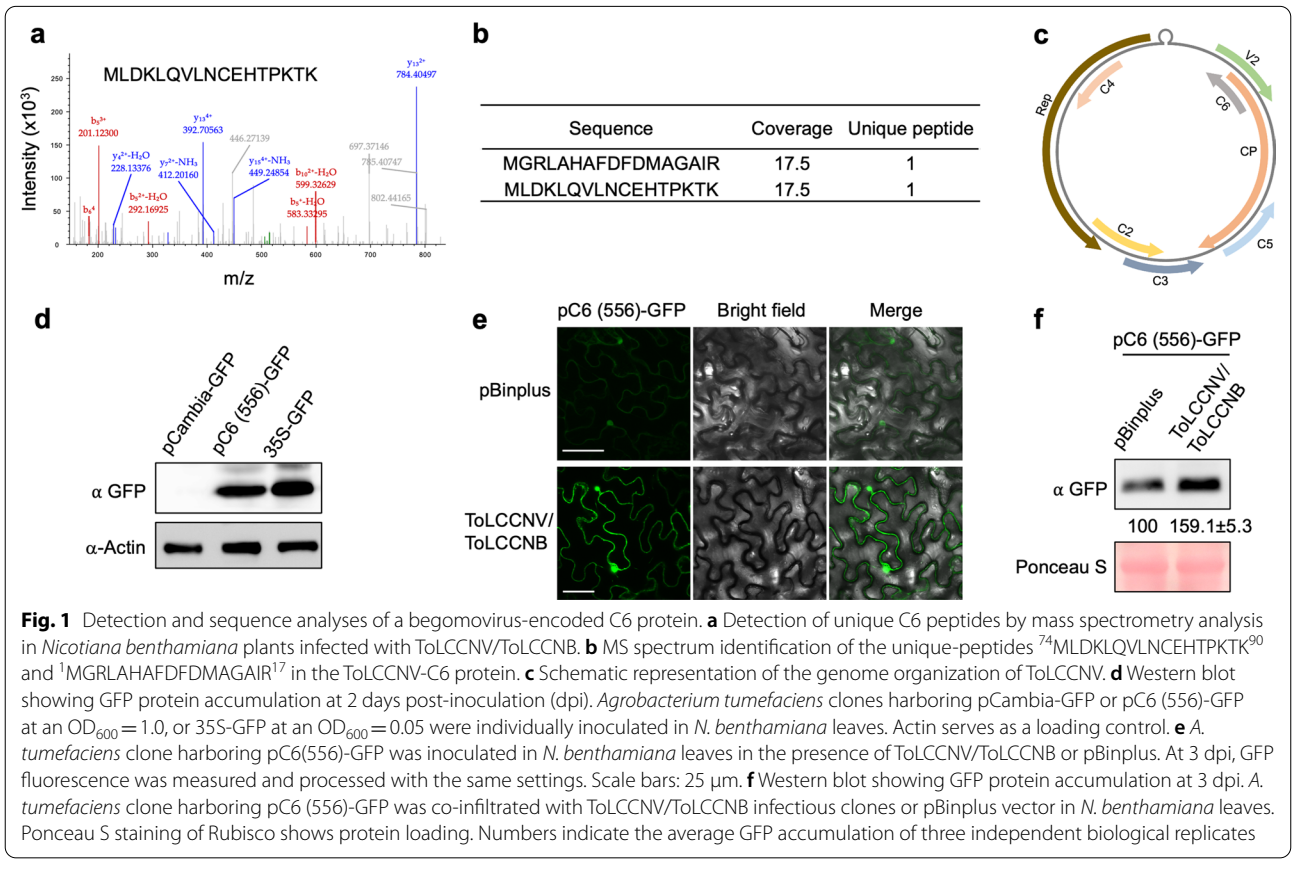

Fig. 1 Detection and sequence analyses of a begomovirus-encoded C6 protein. **a** Detection of unique C6 peptides by mass spectrometry analysis in *Nicotiana benthamiana* plants infected with ToLCCNV/ToLCCNB. **b** MS spectrum identification of the unique-peptides ^{74}MLDKLQVLNCEHTPKTK^{90} and ^{1}MGRLAHAFDFDMAGAIR^{17} in the ToLCCNV-C6 protein. **c** Schematic representation of the genome organization of ToLCCNV. **d** Western blot showing GFP protein accumulation at 2 days post-inoculation (dpi). *Agrobacterium tumefaciens* clones harboring pCambia-GFP or pC6 (556)-GFP at an OD_{600} = 1.0, or 35S-GFP at an OD_{600} = 0.05 were individually inoculated in *N. benthamiana* leaves. Actin serves as a loading control. **e** *A. tumefaciens* clone harboring pC6(556)-GFP was inoculated in *N. benthamiana* leaves in the presence of ToLCCNV/ToLCCNB or pBinplus. At 3 dpi, GFP fluorescence was measured and processed with the same settings. Scale bars: 25 μm. **f** Western blot showing GFP protein accumulation at 3 dpi. *A. tumefaciens* clone harboring pC6 (556)-GFP was co-infiltrated with ToLCCNV/ToLCCNB infectious clones or pBinplus vector in *N. benthamiana* leaves. Ponceau S staining of Rubisco shows protein loading. Numbers indicate the average GFP accumulation of three independent biological replicates

indicating a strengthened C6 promoter activity in the presence of the virus (Fig. 1f).

Phylogenetic analyses of the begomovirus-encoded C6 proteins

Based on the criteria that the predicted ORF locates at the complementary sense of the virus genome, overlaps with the CP and V2 ORFs, and encodes a polypeptide of over 40 amino acids, we identified 154 begomovirus species, which possess an ORF at the same position as ToLCCNV C6, out of 424 begomovirus species (Additional file 1: Table S1). Multiple amino acid sequence alignments of representative potential C6 proteins identified two hydrophobic regions and a positively charged region (Fig. 2a). Notably, the arginine-rich positively charged region of C6 proteins in the Old World begomoviruses is different from that in the New World begomoviruses, which is proline-rich and close to the N-terminus of the protein. Phylogenetic analyses of representative potential C6 proteins also unveiled that C6 proteins from the New World and the Old World begomoviruses were clustered into two separate branches (Fig. 2b). These results indicate that the unexplored C6 gene is evolutionary conserved in the begomovirus lineage.

The C6 protein is localized in mitochondria

To study the subcellular localization of ToLCCNV C6 protein in plant cells, GFP was fused to either the N-terminus (GFP-C6) or the C-terminus of C6 (C6-GFP), and the resulting fusion protein was transiently expressed in *N. benthamiana* leaves. The GFP fluorescence signal for C6, as detected by confocal microscopy, was co-localized with Mito Tracker Red (a mitochondrial fluorescent dye) and AtICP55(N100)-mCherry (a mitochondrial marker) to mitochondria (Carrie et al. 2015) (Fig. 3a, b and Additional file 2: Figure S1a). To further confirm the mitochondrial localization of the C6 protein, immunogold staining of *N. benthamiana* leaf tissues was performed. Gold label was detected in the mitochondria of *N. benthamiana* cells transiently expressing Flag-C6-GFP, while no background labeling was observed with the secondary antibody alone (Fig. 3c). In addition, co-infiltration with ToLCCNV/ToLCCNB had no obvious effect on the mitochondrial localization or protein accumulation of C6 protein at 3 days post-inoculation (dpi) (Additional file 2: Figure S1b). A C6 homologue in another begomovirus, tomato yellow leaf curl China virus (TYLCCNV, GenBank: AJ319675), was detected to be localized in mitochondria as well (Additional file 2: Figure S1c, d). These results collectively provide persuasive evidence that the begomovirus-encoded C6 protein is primarily localized in mitochondria.

Mapping the regions responsible for mitochondrial localization of ToLCCNV C6

Two types of signal peptides, the N-terminal cleavable pre-sequence and the internal non-cleavable sorting signals, which direct proteins from the cytosol into mitochondria have been identified (Chacinska et al. 2009; Schmidt et al. 2010). In silico analysis of ToLCCNV C6 with several prediction tools could not identify any clear N-terminal mitochondrial targeting signals. Consistent with this, N-terminal GFP fusion did not interfere with the mitochondrial localization of C6. To evaluate the contribution of different regions to mitochondrial localization, a series of deletion mutants were generated

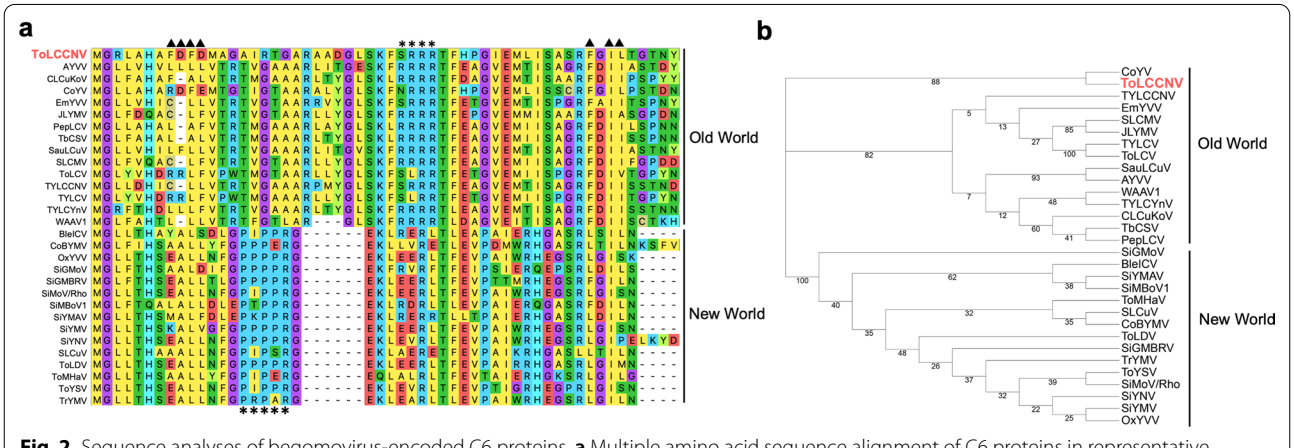

Fig. 2 Sequence analyses of begomovirus-encoded C6 proteins. **a** Multiple amino acid sequence alignment of C6 proteins in representative begomoviruses. Asterisks indicate positively charged regions; triangles indicate hydrophobic regions. **b** Phylogenetic trees constructed based on the amino acid sequences of begomoviruses C6 proteins in **a**. Bootstrap values (%) for 1000 replicates are indicated. Virus names are shown in Additional file 1: Table S3

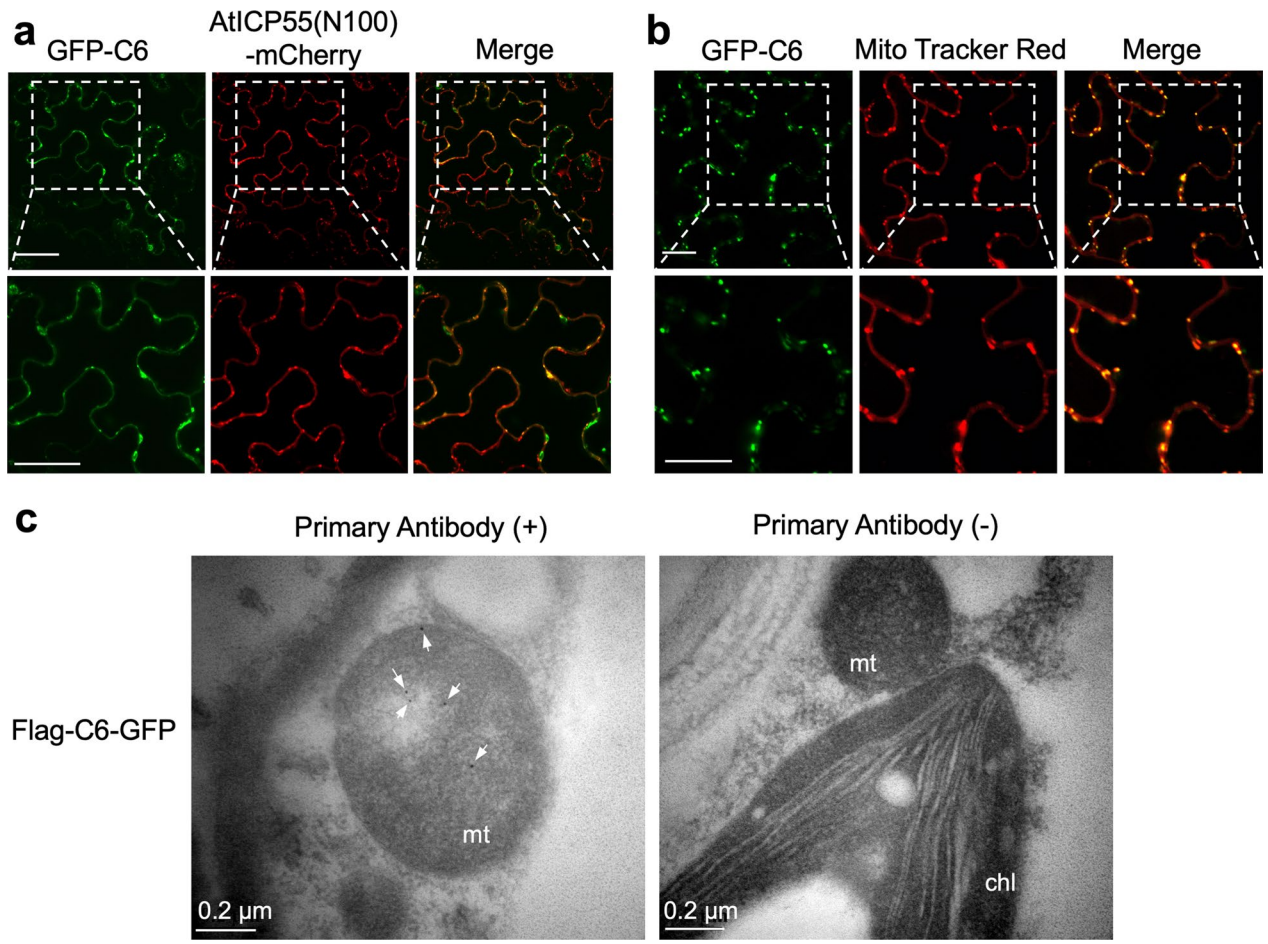

Fig. 3 ToLCCNV C6 protein is localized in the mitochondria of *Nicotiana benthamiana* cells. **a** Co-localization of GFP-C6 with the mitochondrial marker AtICP55(N100)-mCherry in mesophyll cells of *N. benthamiana* leaves. Scale bars: 25 μm. **b** Co-localization of GFP-C6 with the mitochondrial stain Mito Tracker Red. Scale bars: 25 μm. **c** Immunogold staining of Flag-C6-GFP protein in *N. benthamiana* mesophyll cells with (left panel) or without (right panel) GFP antibody. Arrows indicate gold label in the mitochondrion. Scale bars: 0.2 μm. Mt: mitochondrion. Chl: chloroplast

for transient expression in *N. benthamiana*. Confocal microscopy showed that neither the N-terminus (GFP-C6-1-36, GFP-C6-1-49) nor the C-terminus (GFP-C6-50-97, GFP-C6-37-97) of the C6 protein exhibited mitochondrial localization pattern, suggesting an internal sorting signal responsible for targeting mitochondria (Fig. 4). The C6 truncation GFP-C6-30-97 but not GFP-C6-37-97 was localized in mitochondria, indicating the importance of the residues 30–36, which contains a conserved positively charged region, in mitochondrial targeting. However, these residues are not enough to enable the mitochondrial targeting since the C6 truncation that consists of the N-terminal 49 amino acid (GFP-C6-1-49) showed only cytosolic distribution (Fig. 4). These results indicate that an internal conserved positively charged region and a targeting sequence located at the C-terminal region of C6 function synergistically in mediating the mitochondrial localization of the protein.

C6 does not contribute to ToLCCNV virulence towards *N. benthamiana*

In order to test whether C6 is involved in symptom development, the C6 protein was ectopically expressed in *N. benthamiana* plants using a potato virus X (PVX)-based vector. A C6 mutant with two substitutions (GT382CA) that introduce a non-sense mutation at the amino acid position 18 was generated as the negative control (PVX-mC6). At 8 dpi, leaf puckering and chlorosis were observed in both PVX-C6 and PVX-mC6 infected plants (Fig. 5a). Western blot analysis with an antibody against PVX-CP indicated that the accumulation of PVX was comparable between plants infected with PVX-C6 and PVX-mC6 (Fig. 5b, c), suggesting that ToLCCNV C6 could not directly interfere with plant development.

To investigate whether C6 plays a role in ToLCCNV infection, the infectious clone of ToLCCNV with

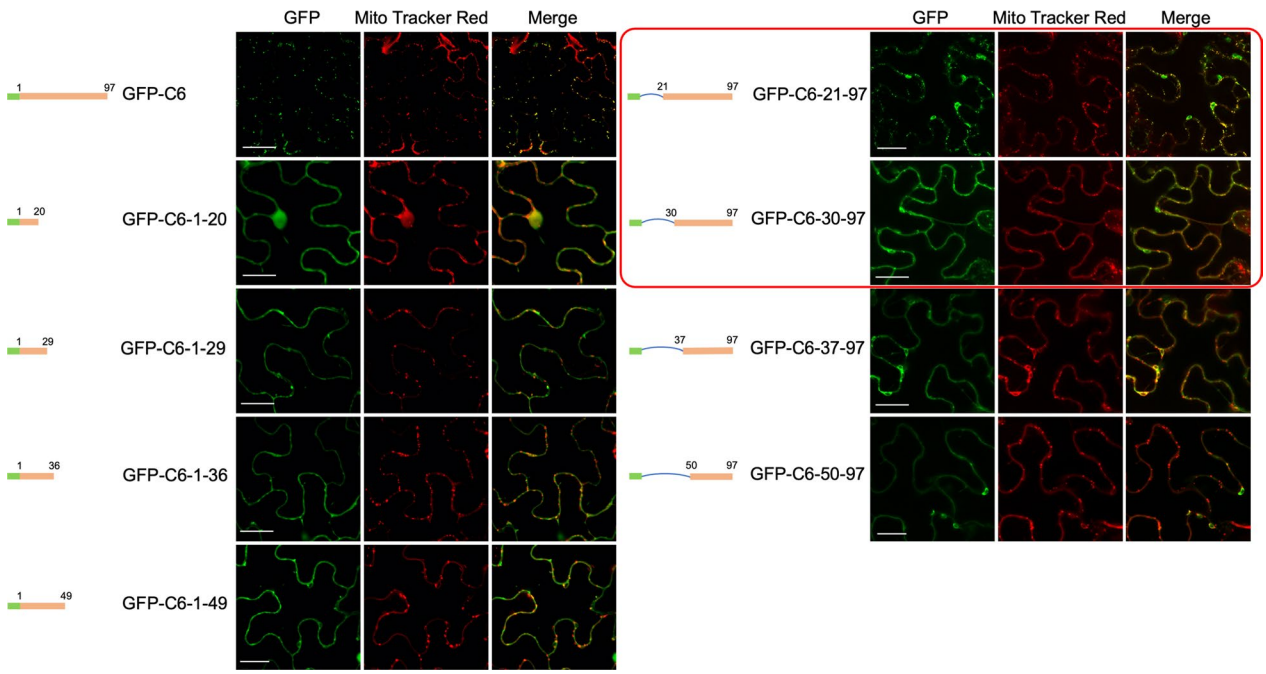

Fig. 4 Subcellular localization patterns of C6-deletion derivatives. Amino acid residues of C6 retained in mutants are indicated. Columns from left to right represent GFP fluorescence, Mito Tracker Red fluorescence and overlay. Scale bars: 25 μm. Rectangle indicates C6 truncations with mitochondrial localization

mutations that render it unable to produce C6 was constructed. Due to the overlapping of C6 ORF with CP and V2 ORFs, we were unable to generate a C6-null mutation without affecting neither CP nor V2 proteins. Therefore, a non-sense mutation in C6 at the amino acid position 18 also resulted in an S86C mutation in CP and a V33H mutation in V2 (ToLCCNV-mC6, Additional file 2: Figure S2a). The resulting ToLCCNV-mC6 was agro-inoculated into *N. benthamiana* together with the infectious ToLCCNB clone. Eight days after inoculation, both wild-type ToLCCNV/ToLCCNB-infected and ToLCCNV-mC6/ToLCCNB-infected plants exhibited strong curling of leaves (Fig. 5d). No statistically differences in the accumulation of virus coat protein and viral load were detected between the wild-type virus-infected and C6 mutant virus-infected *N. benthamiana* plants (Fig. 5e–g). Similar results were observed at 16 dpi (Additional file 2: Figure S2b–e). These data indicate that C6 does not affect ToLCCNV infection in *N. benthamiana*, at least in the conditions tested.

Discussion

An increasing number of studies have identified multiple previously neglected virus-encoded proteins that are produced to facilitate begomovirus infection (Gong et al. 2021). Here, a novel C6 protein was identified through mass spectrometry analysis of ToLCCNV-infected samples. The C6 ORF was identified in 36% begomovirus species with highly conserved amino acid sequences. Phylogenetic analyses further indicate the sequence divergence of C6 proteins between the New World and the Old World begomoviruses. These data strongly suggest that expression of C6 is a widespread feature of begomoviruses.

Due to the limited coding capability of mitochondrial DNA, the vast majority of mitochondrial proteins are encoded by nuclear genes and are synthesized in the cytosol. A large number of mitochondrial proteins are synthesized as preproteins with cleavable signal presequences while others contain targeting information in their mature sequences. The internal mitochondrial targeting sequences that lack consistent patterns are still not well characterized (Schmidt et al. 2010). In this study, confocal microscopy, together with in silico analysis, showed that the mitochondrial targeting in C6 protein was not mediated by an N-terminal signal sequence. Instead, the C6 truncations GFP-C6-21-97 and GFP-C6-30-97, which contain a conserved positively charged residues ^{31}RRR^{33} and a targeting sequence at the C-terminal region of the protein, showed mitochondrial localization. Further mutation analysis will help to evaluate and refine the internal regions responsible for targeting of C6 to mitochondria.

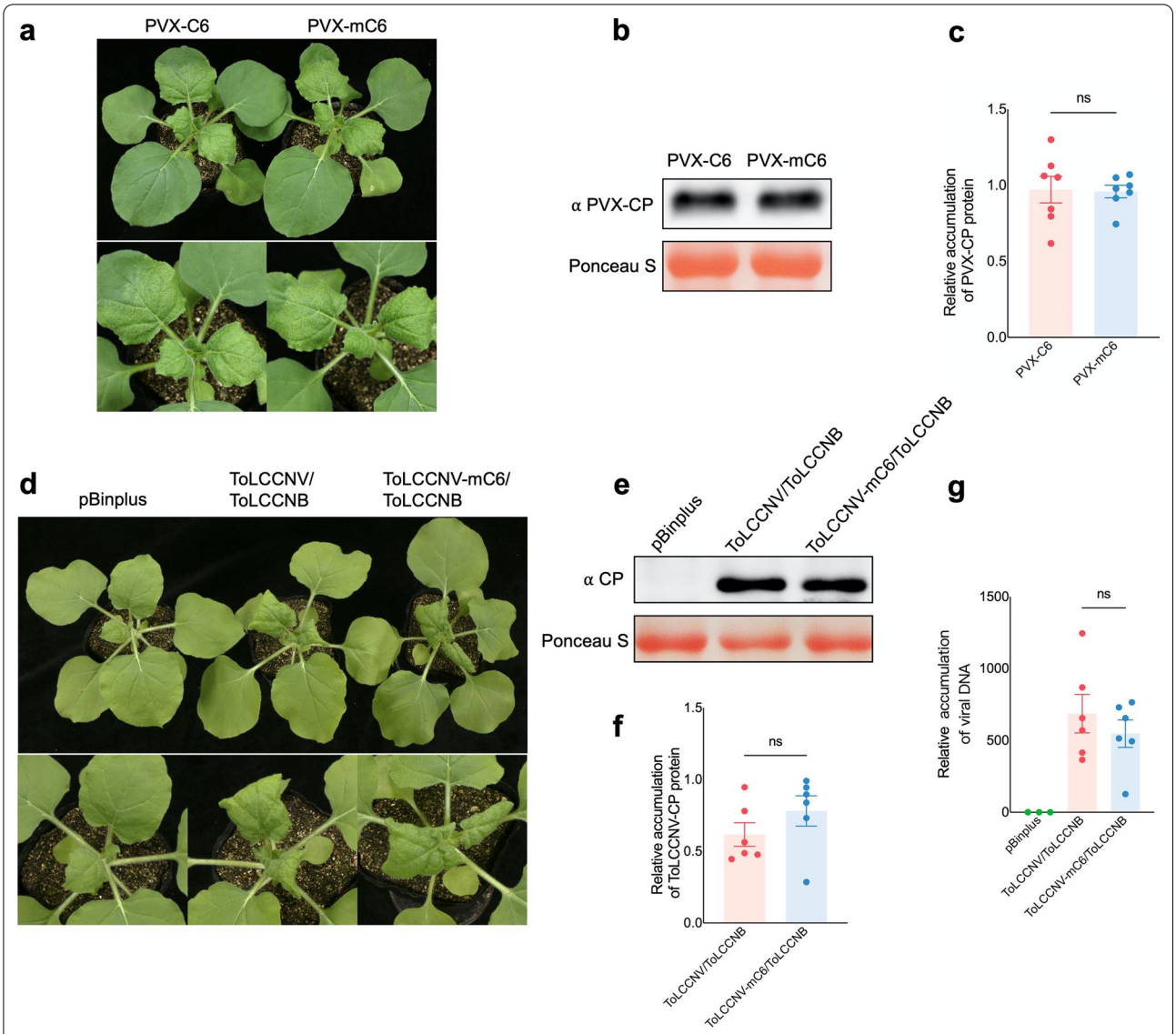

Fig. 5 ToLCCNV C6 protein is dispensable for virulence. **a** Symptoms in *Nicotiana benthamiana* plants at 8 days post-inoculation (dpi) with PVX-C6 or PVX-mC6. **b** Western blot analysis of PVX coat protein (PVX-CP) accumulation in plants infected with PVX-C6 or PVX-mC6. Ponceau S staining of Rubisco shows protein loading. **c** Quantification of PVX-CP accumulation in plants infected with PVX-C6 or PVX-mC6, analyzed from the Western blot images using Image J. Data are the mean of seven independent biological replicates. **d** Symptoms of *N. benthamiana* plants infected with ToLCCNV/ToLCCNB, ToLCCNV-mC6/ToLCCNB, or control (pBinplus) at 8 dpi. **e** Western blot analysis of ToLCCNV coat protein (CP) accumulation in systemic leaves shown in **d**. Ponceau S staining of Rubisco shows protein loading. **f** Quantification of CP accumulation in *N. benthamiana* plants infected with ToLCCNV/ToLCCNB or ToLCCNV-mC6/ToLCCNB, analyzed from the Western blot images using Image J. Data are the mean of six independent biological replicates. **g** Viral DNA accumulation in ToLCCNV/ToLCCNB, ToLCCNV-mC6/ToLCCNB infected or control (pBinplus) plants in **d**, measured by qPCR. Data are the mean of six independent biological replicates. Error bars represent standard deviation (SD). ns, no significant difference (Student's *t*-test; $P \geq 0.05$). *NbActin* was used as an internal reference

Mitochondria are dynamic organelles involved in a wide range of cellular processes, such as energy metabolism, calcium homeostasis, cell death, and innate immune signaling. Induced mitochondrial alternative oxidase (AOX) pathway promotes a systemic basal defense against tobacco mosaic virus (TMV) infection (Liao et al. 2012). However, how mitochondria react upon begomovirus infection and whether viruses affect mitochondrial functions remain elusive. Although in our hand, the C6-null mutant version of ToLCCNV and the wild-type ToLCCNV induced identical symptom, it is still possible that the C6 protein could modify host mitochondrial functions during viral infection. Further examination of the location of C6 in separated mitochondrial fractions and screening

of mitochondrial components that interact with C6 will help in understanding the function of C6.

Conclusions

We identified a novel begomovirus-encoded protein, C6, which is evolutionarily conserved and localized in mitochondria. The identification and subcellular localization of C6 will provide a basis for further structure-function studies.

Methods

Plasmids and constructs

The coding sequences of the ToLCCNV-C6, TYLCCNV-C6, and AtICP55 genes were subcloned into the pClone007 vector (TsingKe, Beijing, CN). Plant expression constructs (pCambia-GFP-MCS, pCambia-MCS-GFP, pCambia-Flag-MCS, pGR106, and pBinplus) were digested, and C6 or its deletion mutants were inserted into the vector by T4 DNA ligase (Thermofisher, Waltham, the USA) or ClonExpress II One Step Cloning Kit (Vazyme, Nanjing, CN). To generate site-directed mutagenesis of virus infectious clones, the sequence of ToLCCNV was cloned into pClone007 vector and the construct was amplified with the primer pair (pBin-mC6-F/pBin-mC6-R) to introduce the ToLCCNV-mC6 point mutation, generating pClon007-ToLCCNV-mC6. The sequence of ToLCCNV-mC6 was digested with two different sets of endonucleases and cloned into pBinplus to generate ToLCCNV-mC6 infectious clone. Primers used in this study are listed in Additional file 1: Table S2.

Virus genome sequence analysis

Sequences of begomovirus species were obtained from the International Committee on Taxonomy of Viruses (https://ictv.global/report/chapter/geminiviridae/geminiviridae/begomovirus) and GenBank database (https://www.ncbi.nlm.nih.gov/genbank). ORFs were predicted and analyzed using SnapGene. Multiple amino acid sequence alignments were performed using MUSCLE in MEGA X (https://www.megasoftware.net/). Phylogenetic analyses were performed using the maximum likelihood method in MEGA X and Jones–Taylor–Thornton (JTT) model with 1000 bootstrap replicates. The GenBank accession numbers of sequences analyzed in the study are listed in Additional file 1: Table S3.

Agroinfiltration and virus inoculation

Plant expression constructs were transformed into *Agrobacterium tumefaciens* strains EHA105 (for transit expression and virus infection) and GV3101 (for PVX-vector expression). For virus inoculation, *A. tumefaciens* cultures carrying infectious clones of ToLCCNV, ToLCCNB, ToLCCNV-mC6, or pBinplus empty vector at an $OD_{600}=1.0$ were infiltrated into the leaves of *N. benthamiana* plants at the eight-leaf stage. For recombinant PVX vectors expressing C6 or C6 non-sense mutant, each *A. tumefaciens* culture was infiltrated into the leaves of *N. benthamiana* plants at the eight-leaf stage. Plants were then maintained in a growth chamber at 25 °C under a 14-h light/10-h dark photoperiod.

Mass spectrometry analysis

At 15 dpi, total protein of *N. benthamina* plants infected with ToLCCNV/ToLCCNB was extracted with protein extraction buffer (40 mM Tris-HCl, pH 7.5, 150 mM NaCl, 5 mM MgCl2, 2 mM EDTA, 5 mM DTT, 0.1% Triton X-100, 2% glycerol, 2mM PMSF, and protease inhibitor mixture), centrifuged for 10 min at 8000 *g*, and the soluble proteins were subjected for mass spectrometry analysis. Polypeptides encoded by potential virus ORFs with length over 20 amino acids were collected to establish a protein database for the peptide-mapping searching.

DNA isolation and real-time quantitative PCR (qPCR)

Young leaf tissues from inoculated *N. benthamiana* plants were harvested at indicated days post-inoculation. Total DNA was extracted using hexadecyltrimethylammonium bromide (CTAB) method. qPCR was conducted using LightCycler 480 (Roche, Rotkreuz, Switzerland) with SYBR Premix EX Taq (TaKaRa, Kyoto, Japan). Primer sequences are listed in Additional file 1: Table S2.

Western blot analysis

Total proteins were separated in SDS-PAGE gel and transferred to nitrocellulose membranes (GE Healthcare, Chicago, IL, USA). Membranes were incubated with specific primary antibodies against GFP or Actin (ABclonal, Wuhan, China). Monoclonal antibodies against PVX CP or ToLCCNV CP were generated in our lab. Horseradish peroxidase-conjugated goat anti-mouse IgG (Invitrogen, Carlsbad, CA, US) was used as the secondary antibody. ECL prime Western blot detection reagent (4A Biotech, Beijing, China) was added to the membranes for chemiluminescence detection using ImageQuant LAS 4000 mini (GE Healthcare, Chicago, IL, USA).

Confocal microscopy

For subcellular localization assays, *A. tumefaciens* clones harboring designated constructs were infiltrated separately into the leaves of *N. benthamiana* plants at the eight-leaf stage. Subcellular localization was determined at 2 dpi under a laser scanning confocal microscope FV3000 (Olympus). The excitation wavelengths

of GFP, mCherry, and Mito Tracker Red signals were set to 488, 532, and 579 nm, respectively. Mito Tracker Red was infiltrated into *N. benthamiana* leaves at 2 h before observation. Samples were imaged using a confocal microscope with laser excitation at 488 nm and emission at 512–527 nm.

Immunogold labeling and transmission electron microscopy (TEM) imaging

Leaf tissues of *N. benthamiana* plants transiently expressed with Flag-C6-GFP were fixed in 100 mM phosphate buffered saline (PBS; pH 7.2) containing 0.1% (vol/vol) glutaraldehyde and 3% (vol/vol) formaldehyde for 2 h. The samples were rinsed with 100 mM PBS and dehydrated in a graded ethanol series (50, 70, 90, 100, 100, and 100%), and then embedded in Lowicryl K4M resin (Electron Microscopy Sciences, Fort Washington, PA, USA). After cut into ultrathin sections, the samples were mounted onto nickel grids. For immunogold labeling and TEM imaging, the grids were incubated in blocking solution (BL) (50 mM PBS (pH 7.2) containing 1.0% bovine serum albumin and 0.02% polyethylene glycol 2000) for 30 min at room temperature, and then incubated for 1 h in GFP polyclonal antibody diluted in BL for 1 h at room temperature. The grids were washed with PBS and then incubated with Protein A-gold (Sigma, St. Louis, MO, USA) diluted in BL for 1 h. After incubation, the grids were washed with PBS and sterile ddH_2O, stained with uranyl acetate and lead citrate, and examined using an electron microscope (JEM-1200EX; JEOL, Japan). The control experiment was processed without the presence of primary antibody.

Abbreviations

CP: Coat protein; dpi: Days post-inoculation; GFP: Green fluorescent protein; aa: Amino acid; MP: Movement protein; MS: Mass spectrometry; NSP: Nuclear shuttle protein; PTGS: Post-transcriptional gene silencing; PVX: Potato virus X; Ren: Replication enhancer protein; Rep: Replication-associated protein; ssDNA: Single-stranded DNA; TEM: Transmission electron microscopy; TGS: Transcriptional gene silencing; ToLCCNB: Tomato leaf curl China betasatellite; ToLCCNV: Tomato leaf curl China virus; TrAP: Transcription activator protein.

Supplementary Information

The online version contains supplementary material available at https://doi.org/10.1186/s42483-022-00151-z.

Additional file 1: Table S1. Begomovirus species that possess the potential C6 ORF. **Table S2.** Primers used in this study. **Table S3.** GenBank accession numbers of sequences analyzed in the study.

Additional file 2: Figure S1. Intracellular distribution of ToLCCNV-C6 and TYLCCNV-C6 in *Nicotiana benthamiana* cells. **Figure S2.** The C6 protein of ToLCCNV has no virulence function.

Acknowledgements

The authors wish to thank Dr. Li Xie (Zhejiang University) for help with the immunogold labeling analysis and Yunqin Li (Zhejiang University) for providing technical support of confocal microscopy.

Authors' contributions

XZ conceived and designed the study; ZW, YW, and TH conducted the experiments; ZW and TH analyzed the data; ZW, RLD, TH, and XZ wrote the manuscript. All authors read and approved the final manuscript.

Funding

This work was financially supported by the National Natural Science Foundation of China (31720103914 and 32001866).

Availabilityof data and materials

The datasets used and/or analyzed during the current study are available from the corresponding author on reasonable request.

Declarations

Ethics approval and consent to participate

Not applicable.

Consent for publication

Not applicable.

Competing interests

The authors declare that they have no competing interests.

Author details

[1]State Key Laboratory of Rice Biology, Institute of Biotechnology, Zhejiang University, Hangzhou 310058, China. [2]State Key Laboratory for Biology of Plant Diseases and Insect Pests, Institute of Plant Protection, Chinese Academy of Agricultural Sciences, Beijing 100193, China. [3]Department of Plant Biochemistry, Centre for Plant Molecular Biology (ZMBP), Eberhard Karls University, 72076 Tübingen, Germany.

Received: 14 September 2022 Accepted: 24 November 2022
Published online: 08 December 2022

References

Brown JK, Zerbini FM, Navas-Castillo J, Moriones E, Ramos-Sobrinho R, Silva JCF, et al. Revision of Begomovirus taxonomy based on pairwise sequence comparisons. Arch Virol. 2015;160:1593–619. https://doi.org/10.1007/s00705-015-2398-y.

Carrie C, Venne AS, Zahedi RP, Soll J. Identification of cleavage sites and substrate proteins for two mitochondrial intermediate peptidases in *Arabidopsis thaliana*. J Exp Bot. 2015;66:2691–708. https://doi.org/10.1093/jxb/erv064.

Chacinska A, Koehler CM, Milenkovic D, Lithgow T, Pfanner N. Importing mitochondrial proteins: machineries and mechanisms. Cell. 2009;138:628–44. https://doi.org/10.1016/j.cell.2009.08.005.

Chiu CW, Li YR, Lin CY, Yeh HH, Liu MJ. Translation initiation landscape profiling reveals hidden open-reading frames required for the pathogenesis of tomato yellow leaf curl Thailand virus. Plant Cell. 2022;34:1804–21. https://doi.org/10.1093/plcell/koac019.

Fiallo-Olivé E, Lett M, Martin DP, Roumagnac P, Varsani A, Zerbini FM, et al. ICTV virus taxonomy profile: *Geminiviridae*. J Gen Virol. 2021;102:001696. https://doi.org/10.1099/jgv.0.001696.

Fondong VN. Geminivirus protein structure and function: geminivirus proteins. Mol Plant Pathol. 2013;14:635–49. https://doi.org/10.1111/mpp.12032.

Fontenelle MR, Luz DF, Gomes APS, Florentino LH, Zerbini FM, Fontes EP. Functional analysis of the naturally recombinant DNA-A of the bipartite begomovirus Tomato chlorotic mottle virus. Virus Res. 2007;126:262–7. https://doi.org/10.1016/j.virusres.2007.02.009.

Gong P, Tan H, Zhao S, Li H, Liu H, Ma Y, et al. Geminiviruses encode additional small proteins with specific subcellular localizations and virulence function. Nat Commun. 2021;12:4278. https://doi.org/10.1038/s41467-021-24617-4.
Gong P, Zhao S, Liu H, Chang Z, Li F, Zhou X. Tomato yellow leaf curl virus V3 protein traffics along microfilaments to plasmodesmata to promote virus cell-to-cell movement. Sci China Life Sci. 2022;65:1046–9. https://doi.org/10.1007/s11427-021-2063-4.
Hanley-Bowdoin L, Settlage SB, Orozco BM, Nagar S, Robertson D. Geminiviruses: models for plant DNA replication, transcription, and cell cycle regulation. Crit Rev Biochem Mol Biol. 2000;35:105–40. https://doi.org/10.1016/S0735-2689(99)00383-4.
Hanley-Bowdoin L, Bejarano ER, Robertson D, Mansoor S. Geminiviruses: masters at redirecting and reprogramming plant processes. Nat Rev Microbiol. 2013;11:777–88. https://doi.org/10.1038/nrmicro3117.
Hu T, Song Y, Wang Y, Zhou X. Functional analysis of a novel βV1 gene identified in a geminivirus betasatellite. Sci China Life Sci. 2020;63:688–96. https://doi.org/10.1007/s11427-020-1654-x.
Laufs J. Geminivirus replication: genetic and biochemical characterization of rep protein function, a review. Biochimie. 1995;77:765–73. https://doi.org/10.1016/0300-9084(96)88194-6.
Lazarowitz SG, Beachy RN. Viral movement proteins as probes for intracellular and intercellular trafficking in plants. Plant Cell. 1999;11:535–48. https://doi.org/10.1105/tpc.11.4.535.
Li F, Xu X, Huang C, Gu Z, Cao L, Hu T, et al. The AC5 protein encoded by mungbean yellow mosaic India virus is a pathogenicity determinant that suppresses RNA silencing-based antiviral defenses. New Phytol. 2015;208:555–69. https://doi.org/10.1111/nph.13473.
Li F, Yang X, Bisaro DM, Zhou X. The βC1 protein of geminivirus–betasatellite complexes: a target and repressor of host defenses. Mol Plant. 2018;11:1424–6. https://doi.org/10.1016/j.molp.2018.10.007.
Li P, Su F, Meng Q, Yu H, Wu G, Li M, et al. The C5 protein encoded by ageratum leaf curl Sichuan virus is a virulence factor and contributes to the virus infection. Mol Plant Pathol. 2021;22:1149–58. https://doi.org/10.1111/mpp.13103.
Liao Y, Shi K, Fu L, Zhang S, Li X, Dong D, et al. The reduction of reactive oxygen species formation by mitochondrial alternative respiration in tomato basal defense against TMV infection. Planta. 2012;235:225–38. https://doi.org/10.1007/s00425-011-1483-z.
Pooma W, Petty ITD. Tomato golden mosaic virus open reading frame AL4 is genetically distinct from its C4 analogue in monopartite geminiviruses. J Gen Virol. 1996;77:1947–51. https://doi.org/10.1099/0022-1317-77-8-1947.
Rojas MR, Jiang H, Salati R, Xoconostle-Cázares B, Sudarshana MR, Lucas WJ, et al. Functional analysis of proteins involved in movement of the monopartite begomovirus, Tomato yellow leaf curl virus. Virology. 2001;291:110–25. https://doi.org/10.1006/viro.2001.1194.
Rybicki EP. A phylogenetic and evolutionary justification for three genera of Geminiviridae. Arch Virol. 1994;139:49–77. https://doi.org/10.1007/BF01309454.
Schmidt O, Pfanner N, Meisinger C. Mitochondrial protein import: from proteomics to functional mechanisms. Nat Rev Mol Cell Biol. 2010;11:655–67. https://doi.org/10.1038/nrm2959.
Sunter G, Bisaro DM. Transactivation in a geminivirus: AL2 gene product is needed for coat protein expression. Virology. 1991;180:416–9. https://doi.org/10.1016/0042-6822(91)90049-H.
Sunter G, Bisaro DM. Transactivation of geminivirus AR1 and BR1 gene expression by the viral AL2 gene product occurs at the level of transcription. Plant Cell. 1992;4:1321–31. https://doi.org/10.1105/tpc.4.10.1321.
Yang X, Guo W, Li F, Sunter G, Zhou X. Geminivirus-associated betasatellites: exploiting chinks in the antiviral arsenal of plants. Trends Plant Sci. 2019;24:519–29. https://doi.org/10.1016/j.tplants.2019.03.010.
Zerbini FM, Briddon RW, Idris A, Martin DP, Moriones E, Navas-Castillo J, et al. ICTV virus taxonomy profile: *Geminiviridae*. J Gen Virol. 2017;98:131–3. https://doi.org/10.1099/jgv.0.000738.
Zhou X. Advances in understanding begomovirus satellites. Annu Rev Phytopathol. 2013;51:357–81. https://doi.org/10.1146/annurev-phyto-082712-102234.